



American Society of Hematology  
2021 L Street NW, Suite 900,  
Washington, DC 20036  
Phone: 202-776-0544 | Fax 202-776-0545  
editorial@hematology.org

## Kinase-inactivated CDK6 preserves the long-term functionality of adult hematopoietic stem cells

Tracking no: BLD-2023-021985R2

Isabella Mayer (University of Veterinary Medicine, Austria) Eszter Doma (University of Veterinary Medicine, Austria) Thorsten Klampfl (University of Veterinary Medicine Vienna, Austria) Michaela Prchal-Murphy (Veterinary University of Vienna, Austria) Sebastian Kollmann (University of Veterinary Medicine, Austria) Alessia Schirripa (University of Veterinary Medicine, Austria) Lisa Scheiblecker (University of Veterinary Medicine Vienna, Austria) Markus Zojer (University of Veterinary Medicine, Austria) Natalia Kunowska (University of Graz, Austria) Lea Gebrail (University of Veterinary Medicine, Austria) Lisa Shaw (Medical University Vienna, Austria) Ulrike Mann (Medical University of Vienna, Austria) Alex Farr (Medical University of Vienna, Austria) Reinhard Grausenburger (University of Veterinary Medicine Vienna, Austria) Gerwin Heller (Medical University of Vienna, Austria) Eva Zebedin-Brandl (medical university, Austria) Matthias Farlik (Medical University of Vienna, Austria) Marcos Malumbres (Vall d'Hebron Institute of Oncology (VHIO) and ICREA, Spain) Veronika Sexl (University of Innsbruck, Austria) Karoline Kollmann (University of Veterinary Medicine Vienna, Austria)

### Abstract:

Hematopoietic stem cells (HSCs) are characterized by the ability to self-renew and to replenish the hematopoietic system. The cell-cycle kinase cyclin dependent-kinase 6 (CDK6) regulates transcription, whereby it has both kinase-dependent and kinase-independent functions. We here describe the complex role of CDK6, balancing quiescence, proliferation, self-renewal and differentiation in activated HSCs. Mouse HSCs expressing kinase-inactivated CDK6 show enhanced long-term repopulation and homing, whereas HSCs lacking CDK6 have impaired functionality. The transcriptomes of basal and serially transplanted HSCs expressing kinase-inactivated CDK6 exhibit an expression pattern dominated by HSC quiescence and self-renewal, proposing a concept where MAZ and NFY-A are critical CDK6 interactors. Pharmacologic kinase inhibition with a clinically used CDK4/6 inhibitor in murine and human HSCs validated our findings and resulted in increased repopulation capability and enhanced stemness. Our findings highlight a kinase-independent role of CDK6 in long-term HSC functionality. CDK6 kinase inhibition represents a possible strategy to improve HSC fitness.

**Conflict of interest:** No COI declared

**COI notes:**

**Preprint server:** No;

**Author contributions and disclosures:** Conceptualization, I.M.M., T.K., E.D., V.S., K.K.; formal analysis, T.K., M.Z., R.G., G.H.; performing experiments I.M.M., E.D., S.K., L.S., M.P-M., A.S., M.F.; technical support U.M., L.E.S., N.K; resources: M.M.; A.F., E.Z-B.; writing, I.M.M., E.D., T.K., K.K.; supervision, V.S., K.K.

**Non-author contributions and disclosures:** No;

**Agreement to Share Publication-Related Data and Data Sharing Statement:** Low-input RNA-seq data are available at GEO under accession number E-MTAB-13145 or with the link <https://www.ebi.ac.uk/biostudies/arrayexpress/studies/E-MTAB-13145?key=ab2083d3-92c0-4cf9-ab87-cb4bfb5fb8f7>. ScRNA-seq data of Cdk6+/+, Cdk6KM/KM and Cdk6-/- LSK cells are available at GEO under accession number E-MTAB-13149 or the link <https://www.ebi.ac.uk/biostudies/arrayexpress/studies/E-MTAB-13149?key=1c62daa4-fe2b-442a-a1e0-9840d5c0c00a>. ScRNA-seq data of Palbociclib or Ctrl pre-treated LSK cell are available at GEO under accession number E-MTAB-13268 or the link <https://www.ebi.ac.uk/biostudies/arrayexpress/studies/E-MTAB-13268?key=6f57d2b2-99d3-4c6b-b088-2b7f9fbc6967>.

**Clinical trial registration information (if any):**

**Kinase-inactivated CDK6 preserves the long-term functionality  
of adult hematopoietic stem cells**

Isabella M. Mayer<sup>1</sup>, Eszter Doma<sup>1</sup>, Thorsten Klampfl<sup>1</sup>, Michaela Prchal-Murphy<sup>1</sup>, Sebastian Kollmann<sup>1</sup>, Alessia Schirripa<sup>1</sup>, Lisa Scheiblecker<sup>1</sup>, Markus Zojer<sup>1</sup>, Natalia Kunowska<sup>2</sup>, Lea Gebrail<sup>1</sup>, Lisa E. Shaw<sup>3</sup>, Ulrike Mann<sup>3</sup>, Alex Farr<sup>4</sup>, Reinhard Grausenburger<sup>1</sup>, Gerwin Heller<sup>5</sup>, Eva Zebedin-Brandl<sup>6</sup>, Matthias Farlik<sup>3</sup>, Marcos Malumbres<sup>7-9</sup>, Veronika Sexl<sup>1,10</sup>, Karoline Kollmann<sup>1,\*</sup>

<sup>1</sup>University of Veterinary Medicine Vienna, Department of Biological Sciences and Pathobiology, Pharmacology and Toxicology, 1210 Vienna, Austria

<sup>2</sup>University of Graz, Pharmaceutical Chemistry, Institute of Pharmaceutical Sciences, 8010 Graz, Austria

<sup>3</sup>Medical University of Vienna, Department of Dermatology, 1090 Vienna Austria

<sup>4</sup>Medical University of Vienna, Department of Obstetrics and Gynecology, 1090 Vienna Austria

<sup>5</sup>Medical University of Vienna, Department of Medicine I, Clinical Division of Oncology, 1090 Vienna, Austria

<sup>6</sup>Medical University of Vienna, Institute of Pharmacology, Centre of Physiology and Pharmacology, 1090 Vienna Austria

<sup>7</sup>Vall d'Hebron Institute of Oncology (VHIO), Cancer Cell Cycle group, 08035 Barcelona, Spain

<sup>8</sup>Spanish National Cancer Research Center (CNIO), Cell Division and Cancer group, 28029 Madrid, Spain.

<sup>9</sup>ICREA, 08010 Barcelona, Spain

<sup>10</sup>University of Innsbruck, 6020 Innsbruck, Austria

\*Lead contact

**\*Correspondence:** karoline.kollmann@vetmeduni.ac.at

Low-input RNA-seq data are available at GEO under accession number E-MTAB-13145 or with the link <https://www.ebi.ac.uk/biostudies/arrayexpress/studies/E-MTAB->

13145?key=ab2083d3-92c0-4cf9-ab87-cb4bfb5fb8f7. ScRNA-seq data of Cdk6+/+, Cdk6KM/KM and Cdk6-/- LSK cells are available at GEO under accession number E-MTAB-13149 or the link <https://www.ebi.ac.uk/biostudies/arrayexpress/studies/E-MTAB-13149?key=1c62daa4-fe2b-442a-a1e0-9840d5c0c00a>. ScRNA-seq data of Palbociclib or Ctrl pre-treated LSK cell are available at GEO under accession number E-MTAB-13268 or the link <https://www.ebi.ac.uk/biostudies/arrayexpress/studies/E-MTAB-13268?key=6f57d2b2-99d3-4c6b-b088-2b7f9fbc6967>.

**Running title:** Kinase-inactivated CDK6 maintains HSC self-renewal

**Key words:** HSC; self-renewal; CDK6; MAZ; kinase inactive;

## Abstract

Hematopoietic stem cells (HSCs) are characterized by the ability to self-renew and to replenish the hematopoietic system. The cell-cycle kinase cyclin dependent-kinase 6 (CDK6) regulates transcription, whereby it has both kinase-dependent and kinase-independent functions. We here describe the complex role of CDK6, balancing quiescence, proliferation, self-renewal and differentiation in activated HSCs. Mouse HSCs expressing kinase-inactivated CDK6 show enhanced long-term repopulation and homing, whereas HSCs lacking CDK6 have impaired functionality. The transcriptomes of basal and serially transplanted HSCs expressing kinase-inactivated CDK6 exhibit an expression pattern dominated by HSC quiescence and self-renewal, proposing a concept where MAZ and NFY-A are critical CDK6 interactors. Pharmacologic kinase inhibition with a clinically used CDK4/6 inhibitor in murine and human HSCs validated our findings and resulted in increased repopulation capability and enhanced stemness. Our findings highlight a kinase-independent role of CDK6

in long-term HSC functionality. CDK6 kinase inhibition represents a possible strategy to improve HSC fitness.

## Key Points

- Inhibiting CDK6 kinase function enhances long-term HSC functionality
- Kinase-inactivated CDK6 and MAZ influence HSC maintenance

## Introduction

HSCs are rare components of the adult bone marrow (BM), where they preserve the hematopoietic pool by self-renewal and differentiation<sup>1-3</sup>. Hematopoietic stem cell transplantation (HSCT) is an essential medical procedure for various hematological diseases<sup>4-6</sup>. Although HSCT is a life-saving process, it comes with several limitations due to graft-versus-host disease or relapse<sup>4,5</sup>. The objective is to use most functional and fittest HSCs for a successful HSCT.

CDK6 controls the exit from the G<sub>1</sub> phase of the cell cycle in all cells. The cell cycle is triggered by binding of CDK6 to D-type cyclins, which activates the kinase function of CDK6 and leads to phosphorylation of the retinoblastoma protein (Rb). Subsequent E2F-mediated transcription causes the cells to exit G<sub>1</sub> and enter the S phase<sup>7</sup>. In addition to phosphorylating Rb, CDK6 regulates the transcription of a range of genes in healthy and malignant cells. It does not itself bind to DNA but interacts with a plethora of transcription factors, either in a kinase-dependent or in a kinase-independent manner<sup>8-13</sup>. Using transgenic CDK6 animal models, has been instrumental in our understanding of the complex interplay of the kinase-

dependent and -independent functions of CDK6 in HSPCs<sup>14,15</sup>. However, we do not understand how CDK6 controls the fate of these cells.

We now report that inactivation of the kinase function of CDK6 leads to an enriched pool of quiescent HSCs with a long-term capacity to repopulate the hematopoietic system. We also show that HSCs containing a kinase-inactivated version of CDK6 retain certain features of stem cells that are lost when the HSCs lack CDK6. Our transcriptomics data provide a model to explain how CDK6 stimulates or represses various transcriptional networks to control the fate of HSCs.

## Methods

### *Serial BM transplantation assays*

5x10<sup>6</sup> BM of *Cdk6*<sup>+/+</sup>, *Cdk6*<sup>-/-</sup> or *Cdk6*<sup>KM/KM</sup> donor cells were transplanted intravenously (*i.v.*) into lethally irradiated CD45.1<sup>+</sup> recipients. The long-term repopulation capacities were evaluated after twelve weeks following transplantation by flow cytometry. 5x10<sup>6</sup> CD45.2<sup>+</sup> donor BM cells were re-injected in lethally irradiated CD45.1<sup>+</sup> recipient mice for up to four rounds.

### *Single and repetitive pI:pC injections*

Mice were injected once intraperitoneally (*i.p.*) with 10 mg/kg polyinosinic:polycytidylic acid (pI:pC). Control mice were injected with the same volume of PBS. Mice were opened 18 hours post-treatment and HSC compartment was analysed.

For repetitive analysis, mice were serially injected *i.p.* in every second day (three times total) with 10 mg/kg pI:pC or PBS. Mice were opened 2 days post 3<sup>rd</sup> injection.

All procedures and breeding were approved by the Ethics and Animal Welfare Committee of the University of Veterinary Medicine, Vienna in accordance with the University's guidelines for Good Scientific Practice and authorized by the Austrian Federal Ministry of Education, Science and Research (BMMWF-68.205/0093-WF/V/3b/2015, 2022-0.404.452, BMMWF-68.205/0112-WF/V/3b/2016, BMBWF-68.205/0103-WF/V/3b/2015 (TP), 2023-0.108.862) in accordance with current legislation. The experimental protocols involving human cord blood samples was approved by the Ethics Committee of the Medical University of Vienna (EK1553/2014).

Other methods are described in detail in supplemental Methods, available on the Blood website





## Results

### CDK6 shapes the HSC transcriptomic landscape in a kinase -dependent and -independent manner

To understand the contribution of kinase-dependent and -independent functions of CDK6 in HSCs, we made use of a kinase-inactivated CDK6 K43M knock-in mouse model (*Cdk6*<sup>KM/KM</sup>)<sup>14</sup>, which was compared to CDK6 wild type (*Cdk6*<sup>+/+</sup>) and CDK6 knockout mice (*Cdk6*<sup>-/-</sup>)<sup>15</sup>. HSPC fractions of *Cdk6*<sup>+/+</sup> and *Cdk6*<sup>KM/KM</sup> mice showed comparable CDK6 protein levels (**Fig. S1A-C**). Although BM cellularity was reduced in *Cdk6*<sup>KM/KM</sup> and *Cdk6*<sup>-/-</sup> mice, LSK cell numbers remained unaffected (**Fig. 1A, S1D**). HSC cell numbers were increased and multipotent progenitor 3/4 (MPP3/4) cell numbers are reduced in the *Cdk6*<sup>KM/KM</sup> mice compared to *Cdk6*<sup>+/+</sup> mice, whereas *Cdk6*<sup>-/-</sup> mice showed reduced MPP2 cell numbers compared to *Cdk6*<sup>+/+</sup> mice (**Fig. 1A**). *Cdk6*<sup>KM/KM</sup> and *Cdk6*<sup>-/-</sup> mice showed significantly increased percentage of the HSC subfraction, while the percentage of LSK and MPP1-4 cells remained unaltered irrespective of the genotype (**Fig. S1E-F**).

To determine underlying transcriptional changes in the HSC compartment, we performed high-resolution 10X genomics single-cell RNA-seq (scRNA-seq) of steady-state BM LSK cells. Data integration identified 11 individual cell clusters, which we annotated according to published marker gene expression (**Fig. 1B, S1G**)<sup>16,17</sup>. Differences in cluster sizes were notable between *Cdk6*<sup>KM/KM</sup> and *Cdk6*<sup>-/-</sup> compared to *Cdk6*<sup>+/+</sup> cells (**Fig. S1H**). In line with the known cell cycle function of CDK6<sup>7,14,15</sup>, the “cell cycle clusters” in *Cdk6*<sup>-/-</sup> and *Cdk6*<sup>KM/KM</sup> samples were smaller compared to the *Cdk6*<sup>+/+</sup> cluster. Flow cytometry analysis of *ex vivo* and cultivated *Cdk6*<sup>-/-</sup> and *Cdk6*<sup>KM/KM</sup> LSK or HSC/MPP1 cells verified reduced proliferation (**Fig. S1I-J**).

The HSPC cluster of the scRNA-seq experiment encompassed approximately 20% of all LSK cells (**Fig. 1B**). To better identify transcriptional patterns in more defined HSPCs, we re-integrated the HSPC cluster and annotated dormant HSCs and differentiation-prone cell states based on published marker genes (**Fig. 1C, S1K**)<sup>16,17</sup>. We found nine HSPC subclusters which exhibited transcriptional alterations particularly in the *Cdk6*<sup>KM/KM</sup> mutant setting when compared to *Cdk6*<sup>+/+</sup> or *Cdk6*<sup>-/-</sup> cells. All *Cdk6*<sup>KM/KM</sup> clusters show a more pronounced effect in size compared to *Cdk6*<sup>-/-</sup> clusters, except the cell cycle cluster. We identified opposing effects of *Cdk6*<sup>KM/KM</sup> and *Cdk6*<sup>-/-</sup> cells within the myeloid (Myel), lymphoid (Lym) and interferon (IFN) HSPC subclusters. *Cdk6*<sup>KM/KM</sup> and *Cdk6*<sup>-/-</sup> samples showed increased dormant HSCs to a similar extent as shown in **Fig.1A (Fig. 1D)**. Strikingly, *Cdk6*<sup>KM/KM</sup> HSCs displayed a unique transcriptional pattern leading to an alternative cluster formation (**Fig. 1E**). Differential gene expression analysis of the dormant HSC subcluster unmasked common and unique up- and downregulated genes in *Cdk6*<sup>KM/KM</sup> and *Cdk6*<sup>-/-</sup> compared to *Cdk6*<sup>+/+</sup> cells (**Fig. 1F**). *Cdk6*<sup>KM/KM</sup> HSCs showed on average a reduced expression of a proliferation gene signature (PSig)<sup>18</sup> compared to *Cdk6*<sup>-/-</sup> and *Cdk6*<sup>+/+</sup> cells (**Fig. 1G**). *Cdk6*<sup>-/-</sup> cells showed a stronger expression of the quiescence associated signature (Qsig)<sup>18</sup> compared to *Cdk6*<sup>KM/KM</sup> and *Cdk6*<sup>+/+</sup> cells. This result aligns with our previously published data, highlighting that the absence of CDK6 impairs HSC exit from their quiescent state, along with decreased response to HSC-specific stress conditions<sup>13</sup>. These data led us to speculate that *Cdk6*<sup>KM/KM</sup> HSCs respond differently to HSC specific stress challenge compared to *Cdk6*<sup>-/-</sup> HSCs. Kinase-inactivated CDK6 fails to phosphorylate, despite the protein being present, which may block other kinases that compensate in a CDK6-deficient setting.

## Kinase-inactivated CDK6 maintains HSPC potential upon long-term challenge

The transcriptional changes found in *Cdk6*<sup>KM/KM</sup> HSCs point towards alterations in interferon (IFN)-response and activation. We thus injected mice with a single dose of polyinosinic:polycytidylic acid (pI:pC) to analyze the activation response in a short-term setting (**Fig. S2A**). To control for the induction of Sca-1 expression by the IFN-STAT1 axis, we decided on an alternative flow cytometry gating strategy including the CD86 marker<sup>19</sup>. Lineage<sup>-</sup> c-kit<sup>+</sup> CD86<sup>+</sup> cell numbers are similar between the three genotypes upon pI:pC treatment (**Fig. S2B**). As under steady state conditions, HSC/MPP1-2 cell numbers were significantly higher in *Cdk6*<sup>KM/KM</sup> compared to *Cdk6*<sup>+/+</sup> mice. This was not detected for the *Cdk6*<sup>-/-</sup> mice (**Fig. S2C**). *Cdk6*<sup>-/-</sup> HSC/MPP1 cells showed reduced G<sub>1</sub> cell cycle entry upon single pI:pC stimulation, in line with published data<sup>13</sup> (**Fig. S2D**).

To test how *Cdk6*<sup>KM/KM</sup> cells respond to multiple inflammation associated challenges, we performed serial pI:pC injections followed by serial plating assays to study long-term self-renewal (**Fig. 2A**).

Serial pI:pC injections resulted in a decreased BM cellularity in *Cdk6*<sup>-/-</sup> and *Cdk6*<sup>KM/KM</sup> mice compared to *Cdk6*<sup>+/+</sup> mice along with decreased *Cdk6*<sup>-/-</sup> LK<sup>+</sup>CD86<sup>+</sup> and HSC/MPP1 cell numbers (**Fig. 2B, S2E**). *Cdk6*<sup>KM/KM</sup> cells displayed intermediate numbers. MPP2-4 cells remained unchanged irrespective of the genotype (**Fig. S2F**). A higher percentage of *Cdk6*<sup>-/-</sup> and *Cdk6*<sup>KM/KM</sup> HSC/MPP1 cells remained in the G<sub>0</sub> and G<sub>1</sub> cell cycle phases (**Fig. 2C**). Our experimental setting was completed by serially plating BM cells into methylcellulose (**Fig. 2A**). Serial BM cell plating revealed significantly elevated *Cdk6*<sup>KM/KM</sup> LSK cell numbers. In contrast, *Cdk6*<sup>-/-</sup> cells showed reduced LSK cell numbers and even more drastically reduced total cell numbers compared to *Cdk6*<sup>+/+</sup> and *Cdk6*<sup>KM/KM</sup> cells (**Fig. 2D-E, S2G**). *Cdk6*<sup>KM/KM</sup> colonies displayed an overall reduction in differentiated cells compared to *Cdk6*<sup>+/+</sup> and *Cdk6*<sup>-/-</sup> controls upon serial plating, yet *Cdk6*<sup>KM/KM</sup> cells were still able to produce myeloid and lymphoid colonies (**Fig. S2H**). The short- and long-term pI:pC data suggest that kinase-

inactivated CDK6 mimics full loss of CDK6 in regards to cell cycle, which can be seen most prominently in a short-term activation setting. However, in a repetitive activation setting, where long-term stem cell properties come into account, kinase-inactivated CDK6 maintained LSK numbers, while loss of CDK6 led to reduced LSK cell numbers. The advantage of *Cdk6*<sup>KM/KM</sup> HSCs comes with only mild expenses regarding the differentiation potential.

### Kinase-inactivated CDK6 enhances HSC homing and self-renewal

Angpt1 was one of the top upregulated genes in *Cdk6*<sup>KM/KM</sup> compared to *Cdk6*<sup>+/+</sup> and *Cdk6*<sup>-/-</sup> cells from the dormant HSC subcluster (**Fig. 3A**). As Angpt1/Tie2 is a critical signalling component for HSC quiescence and homing<sup>20,21</sup>, we tested whether kinase-independent functions of CDK6 affect homing and migration of HSCs (**Fig. S3A**). Sorted LSK cells were plated in a transwell system including stromal cell-derived factor 1α (SDF-1α) as an attractant. No changes in migration of the total LSK compartment was observed. When analyzing HSC/MPP1 cells, *Cdk6*<sup>KM/KM</sup> cells migrated significantly more than *Cdk6*<sup>-/-</sup> HSC/MPP1 cells *in vitro*. Therefore we performed an *in vivo* homing assay. We injected CD45.2<sup>+</sup> LSK cells of *Cdk6*<sup>+/+</sup>, *Cdk6*<sup>-/-</sup> and *Cdk6*<sup>KM/KM</sup> mice *i.v.* into CD45.1<sup>+</sup> recipient mice (**Fig. 3B**). Injected CD45.2<sup>+</sup> LSK and MPP2-4 progenitor cells were similarly present in the BM irrespective of the genotype 18 hours thereafter (**Fig. 3C, S3B**). In contrast, significantly more *Cdk6*<sup>KM/KM</sup> HSC/MPP1 cells homed to the BM compared to *Cdk6*<sup>+/+</sup> and *Cdk6*<sup>-/-</sup> HSC/MPP1 cells.

Self-renewal and homing are processes involved in HSC engraftment. To assess the repopulation capacity of *Cdk6*<sup>KM/KM</sup> HSC/MPP1 cells we serially transplanted BM cells from CD45.2<sup>+</sup> *Cdk6*<sup>+/+</sup>, *Cdk6*<sup>-/-</sup> and *Cdk6*<sup>KM/KM</sup> mice into lethally irradiated CD45.1<sup>+</sup> recipient mice (**Fig. 3D**). From the 2<sup>nd</sup> round of transplantation onwards, we identified significantly higher numbers of donor-derived *Cdk6*<sup>KM/KM</sup> LSK cells compared to *Cdk6*<sup>+/+</sup> and *Cdk6*<sup>-/-</sup> LSK cells

(Fig. 3E-F). This effect was even more pronounced for the HSC/MPP1 cell compartment (Fig. 3G). In contrast to *Cdk6*<sup>KM/KM</sup> cells, *Cdk6*<sup>-/-</sup> LSK and HSC/MPP1 cells significantly declined over serial rounds of transplantation. *Cdk6*<sup>KM/KM</sup> MPP2-4 progenitor cells displayed higher percentages of BM engraftment compared to *Cdk6*<sup>-/-</sup> MPP2-4 cells within all transplantation rounds (Fig. S3C). No significant differences in the MPP2-4 cells were observed between *Cdk6*<sup>KM/KM</sup> and CDK6 wild type cells.

Comparable percentages of myeloid and lymphoid cells were found upon repopulation of *Cdk6*<sup>+/+</sup> and *Cdk6*<sup>KM/KM</sup> cells in the long-term transplantation setting (Fig. 3H). Of note, *Cdk6*<sup>-/-</sup> cells showed a shift from the myeloid to the lymphoid lineage, with the strongest effect observed in the 2<sup>nd</sup> serial transplantation round. This data is in line with the enhanced lymphoid HSPC subcluster identified by the scRNA-seq data (Fig. 1D). No significant alterations were detected in the composition of the peripheral blood (Fig. S3D). To further investigate the functionality of CDK6 kinase-inactivated HSC/MPP1 cells, we performed competitive transplantation assays with *Cdk6*<sup>KM/KM</sup> or *Cdk6*<sup>+/+</sup> BM cells (Fig. 3I). *Cdk6*<sup>KM/KM</sup> HSC/MPP1 cells showed a competitive advantage compared to control counterparts (Fig. 3J). No major differences in the MPP2-4 fractions and LSK cells between *Cdk6*<sup>+/+</sup> and *Cdk6*<sup>KM/KM</sup> were observed (Fig. S3F-G). These results highlight a specific role for kinase-inactivated CDK6 in the repopulation ability of HSCs, which is not mimicked by full loss of CDK6. *Cdk6*<sup>KM/KM</sup> HSCs balance proliferation, differentiation, and self-renewal by a unique transcriptional regulation.

### **Kinase-inactivated CDK6 balances quiescent and activated transcriptional programs of long-term HSCs**

To gain deeper insights into how kinase-inactivated CDK6 protects HSCs during long-term challenge, we performed low-input RNA-seq of flow cytometry sorted serially transplanted

(2<sup>nd</sup> round) HSC/MPP1 cells (**Fig. 4A**). *Cdk6*<sup>KM/KM</sup> and *Cdk6*<sup>-/-</sup> cells showed unique and common transcriptional changes (**Fig. 4B**). As observed in the scRNA-seq analysis, we identified a CDK6 kinase-inactivated, kinase-dependent and CDK6 loss gene set. We first defined gene sets associated with HSC quiescence or HSC activation (**Fig S4A**)<sup>22</sup>. *Cdk6*<sup>KM/KM</sup> and *Cdk6*<sup>+/+</sup> HSC/MPP1 cells displayed a positive enrichment of the quiescent stem cell gene set compared to *Cdk6*<sup>-/-</sup> HSC/MPP1 cells (**Fig. 4C**). This finding reflected the reduced engraftment potential of the *Cdk6*<sup>-/-</sup> HSC/MPP1 cells over *Cdk6*<sup>KM/KM</sup> and *Cdk6*<sup>+/+</sup> HSC/MPP1 cells (**Fig. 3G**). A significant negative enrichment of the activation stem cell gene set was identified for *Cdk6*<sup>KM/KM</sup> and *Cdk6*<sup>-/-</sup> HSC/MPP1 cells compared to *Cdk6*<sup>+/+</sup> HSC/MPP1 cells, which aligns with the proliferation associated gene signature from the dormant HSC cluster (**Fig. 4D, 1G**). These results highlight the importance of kinase-independent effects of CDK6 in maintaining quiescent gene expression patterns, which becomes critical under HSC long-term behavior. The regulation of the *Cdk6*<sup>KM/KM</sup> and *Cdk6*<sup>-/-</sup> quiescent genes is formerly evident under homeostasis, where we identified a different transcriptional pattern of the dormant *Cdk6*<sup>KM/KM</sup> HSC subcluster (**Fig. 1E-G**).

The CDK6 protein lacks a DNA-binding domain and acts as a transcriptional cofactor<sup>7-9,11,14</sup>. To understand how CDK6 regulates HSC self-renewal and maintenance, we performed a transcription factor motif analysis in promoter regions of the differentially expressed activation signature genes between kinase-inactivated CDK6 and wild type CDK6.

NFY and E2F motifs have been revealed as top hits (**Fig. 4E**). When performing a motif enrichment analysis for the comparison of *Cdk6*<sup>-/-</sup> to *Cdk6*<sup>+/+</sup> cells, we identified a similar pattern than *Cdk6*<sup>KM/KM</sup> mutant compared to *Cdk6*<sup>+/+</sup> cells (**Fig. 4F**). These results validated the canonical cell cycle function of CDK6. Our results confirmed published data of NFY-A, showing that it is a critical factor in proliferating HSCs.

We recently described that CDK6 phosphorylates NFY-A at serine position S325 in transformed BCR/ABL<sup>+</sup> cells. Thereby NFY-A is activated for its transcriptional function<sup>10</sup>. To validate a CDK6-NFY-A interaction in hematopoietic progenitor cells, we took advantage of our recently established HPC<sup>LSK</sup> system and generated stem/progenitor cell lines from *Cdk6*<sup>+/+</sup>, *Cdk6*<sup>-/-</sup> and *Cdk6*<sup>KM/KM</sup> mice.<sup>23</sup> Subcellular fractionation analysis revealed that kinase-inactivated and wild type CDK6 protein was comparable in the chromatin and cytoplasmic fractions (**Fig. 4G**) in HPC<sup>LSK</sup> cells, predicting that kinase-inactivated CDK6 interacts with the chromatin in a similar manner as wild type CDK6. Co-immunoprecipitation (Co-IP) confirmed the protein-protein interaction of CDK6 and NFY-A in *Cdk6*<sup>+/+</sup> and *Cdk6*<sup>KM/KM</sup> HPC<sup>LSK</sup> cells (**Fig. 4H**). To better understand the significance of this interaction, we performed NFY-A shRNA knockdown experiments with *Cdk6*<sup>+/+</sup>, *Cdk6*<sup>-/-</sup> and *Cdk6*<sup>KM/KM</sup> HPC<sup>LSK</sup> cells. Upon NFY-A knockdown, *Cdk6*<sup>KM/KM</sup> HPC<sup>LSK</sup> cells responded with an increased cell death compared to *Cdk6*<sup>+/+</sup> and *Cdk6*<sup>-/-</sup> cells (**Fig. S4B-C**). This data is in line with previous reports that NFY-A loss induces apoptosis and CDK6 kinase activity is needed to antagonize p53-responses<sup>10,24,25</sup>.

## Kinase-inactivated CDK6 and MAZ influence HSC maintenance

To identify kinase-inactivated CDK6 interactors maintaining quiescence, we combined motif enrichment analysis with a CDK6 IP-mass spectrometry experiment. We performed motif enrichment analysis of *Cdk6*<sup>KM/KM</sup> and *Cdk6*<sup>-/-</sup> deregulated genes compared to *Cdk6*<sup>+/+</sup> within the quiescent stem cell gene set from and defined *Cdk6*<sup>KM/KM</sup> specific motifs (**Fig. 5A-B, S5A**). We performed a nuclear CDK6 immunoprecipitation followed by mass spectrometry analysis with the hematopoietic progenitor cell line HPC-7<sup>26</sup> (**Fig. 5C**). An overlap of this data with the *Cdk6*<sup>KM/KM</sup> specific motifs highlighted ZNF148, RUNX1 and myc-associated

zinc finger protein (MAZ) as strongest interactors. The MAZ-CDK6 interaction was validated by proximity ligation assays in *Cdk6*<sup>+/+</sup> and *Cdk6*<sup>KM/KM</sup> HSC/MPP1 cells (**Fig. 5D**).

To assess whether CDK6 and MAZ interplay at chromatin, we re-analyzed publicly available ChIP-seq data sets from transformed B-cells.<sup>10,27</sup> 9501 binding sites were identified as common peaks for CDK6 and MAZ (**Fig. 5E-F**). The associated CDK6-MAZ bound genes enriched for pathways related to chromatin modification, transcriptional regulation, and apoptotic signalling (**Fig. S5B**).

The overlap of CDK6-MAZ binding sites with *Cdk6*<sup>KM/KM</sup> genes upregulated in the HSC subcluster of **Figure 1E** identified that approximately 50% of all genes display a common binding site (**Fig. 5G**). Among these 282 genes are several known HSC mediators (**Fig. 5H**)<sup>16,17,22,28</sup>.

Palbociclib (CDK4/6 kinase inhibitor) treatment did not affect MAZ interaction with the promoters of *Mlec*, *Fosb* and *Hmgb2* in *Cdk6*<sup>+/+</sup> HPC<sup>LSK</sup> cells (**Fig. S5C**) but CDK6 kinase activity influences the transcription of *Mlec* and *Fosb* which is abrogated by MAZ knockdown (siMAZ) (**Fig. S5D**).

MAZ knockdown was performed in sorted LSK cells from *Cdk6*<sup>+/+</sup> and *Cdk6*<sup>KM/KM</sup> mice (**Fig. 5I, S5E**). *Cdk6*<sup>KM/KM</sup> cells responded with a decrease in HSC/MPP1 cells compared to controls (**Fig. 5J-K**). Palbociclib treated *Cdk6*<sup>+/+</sup> LSKs with siMAZ gave comparable results and reduced HSC/MPP1 numbers. The LSK cell fraction remained unaltered in the different conditions (**Fig. S5F**). In summary, this data point at a critical role of the kinase-inactivated CDK6-MAZ axes for HSC maintenance.

### CDK4/6 kinase inhibition protects HSC fitness

We made use of Palbociclib to evaluate its effects on *Cdk6*<sup>+/+</sup> LSK cells by using 10X genomics scRNA-Seq (**Fig. 6A**).



The integrated data identified 13 individual clusters, which we annotated according to published marker gene expression (**Fig. 6B, S6A**)<sup>16,17</sup>. We further sub-structured the HSPC cluster and annotated 4 either immature (naïve) or differentiation-prone cell states (**Fig. 6C, S6B**)<sup>16,17</sup>. In line with the *Cdk6*<sup>KM/KM</sup> HSC subcluster (**Fig. 1D**), the Palbociclib treated sample showed a relative increase in cell number of the naïve subcluster compared to Ctrl (**Fig. 6D**). To study the above defined HSC mediators regulated by CDK6 and MAZ (**Fig. 5G-H**), we analysed the expression of these genes in the naïve subcluster (**Fig. 6E, S6C**). Top genes identified in **Fig. 5H** including *Runx1*, *Cd53*, *Stat3*, *Mlec* and *Cdkn1b*, were found among the top upregulated genes in the naïve Palbociclib treated subcluster compared to control. To compare Palbociclib treated LSK cells with CDK6 kinase-inactive cells, we performed an *in vivo* homing assay. CD45.2<sup>+</sup> *Cdk6*<sup>+/+</sup> LSK cells pre-treated with Palbociclib or control were injected *i.v.* into CD45.1<sup>+</sup> recipient mice (**Fig. S6D-E**). 18 hours upon injection, significantly more HSC/MPP1 cells homed in the BM of the Palbociclib pre-treated setting, while LSK cells remained unchanged. MPP2 cells were increased upon Palbociclib treatment, whereas MPP3-4 were unaltered. To validate the effects of CDK6 kinase inhibition on the colony-forming potential of HSPCs, we performed serial plating assays with Palbociclib (**Fig. S6F**). Palbociclib treatment resulted in increased colony and LSK cell numbers and decreased differentiated cells from the second round of plating onwards. *In vivo* treatment with Palbociclib every 24 hours over 10 days resulted in a higher percentage of HSC/MPP1-MPP2 cells and reduced MPP3/4 cells in the BM (**Fig. 6F,G, S6G-H**). Reduced myeloid cells in the BM confirmed the effectiveness of the treatment (**Fig. S6I**)<sup>29</sup>. HSC/MPP1 cells were embedded for a serial plating assay. Upon the second round of plating, colony and LSK cell numbers of Palbociclib treated mice were enhanced (**Fig. 6H and S6J-K**).

In combination with a MAZ knockdown, the colony numbers were reduced in the Palbociclib and control condition whereas the LSK cells were reduced in the Palbociclib samples (**Fig. S6L-M**).

Further, we treated freshly isolated LSK cells either with Palbociclib (CD45.2) or PBS (CD45.1) and injected in a 1:1 ratio together with carrier bone marrow cells (GFP+) into lethally irradiated recipient mice (**Fig. 6I**). After 16 weeks, Palbociclib treated HSC/MPP1 cells showed a competitive advantage (**Fig. 6J-K, S6N-O**).

To test the effect of Palbociclib in a human setting. CD34<sup>+</sup> cord blood cells were plated with either Palbociclib or control in methylcellulose for serial plating assays (**Fig. 6L**). CD34<sup>+</sup>CD38<sup>-</sup> cells were enriched with Palbociclib (**Fig. 6M-N**). Percentage of CD11b<sup>+</sup> cells was unaltered (**Fig. S6P**).

Taken together, we show that sustaining kinase-independent functions of CDK6 in HSCs enables enhanced long-term capacity, which is reflected in a specific transcriptional pattern. Kinase-inactivated CDK6 regulates quiescent and activated stem cell gene sets at least partially with NFY-A and MAZ.

## Discussion

The function of the hematopoietic system critically depends on the supply of new cells, which are generated as needed by activation of the HSCs. Many patients suffer from hematopoietic deficiencies, but we lack knowledge of when and how to intervene. HSCT is a potentially curative therapy for various hematopoietic diseases. To enhance the success rate of HSCT, we need to maintain stem cell potential and/or improve homing efficiency.

Homing is one of multiple processes involved in engraftment, which seems to be partially influenced by CDK6<sup>30</sup>. We propose that CDK4/6 kinase inhibitors could be used to maintain cultured HSCs in their non-cycling and naïve state before they are transferred to the recipient. While the canonical functions of both CDK4 and CDK6 are inhibited, the kinase-independent functions of CDK6 are generally unaffected or even improved. CDK4/6 inhibitors cause a transient arrest of the cell cycle in HSCs, thereby shield them from chemotherapy induced damages<sup>31</sup>. We suggest that they could be used to treat donor-derived HSCs before HSCT to inhibit their proliferation while improving their regeneration and homing potential.

Critical functions of CDK6 have been described in human cord blood cells. CDK6 enforced expression in long-term (LT) HSCs leads to an increased cell division and those cells acquire a competitive advantage which is suggested to be independent of cyclin expression<sup>32</sup>. Loss of CDK6 in HSCs inhibits the cells' exit from dormancy upon activation<sup>13</sup>. We now demonstrate that kinase-inactivated CDK6 influences the transcription of a set of genes to enhance HSC functionality upon long-term activation. These kinase-independent functions of CDK6 might partially explain the effects of LT-HSCs with enforced CDK6 expression, when cyclins are not expressed yet<sup>32,33</sup>. Loss of CDK6 in HSCs shows the opposite effect.

Hu et al. found 50% reduction in LSK cells of *Cdk6*<sup>-/-</sup> and *Cdk6*<sup>KM/KM</sup> mice compared to *Cdk6*<sup>+/+</sup> mice<sup>14</sup>, while our analysis failed to detect these differences. This could be caused by Sca-1 expression changes. Sca-1 has previously been recognized to react to certain biological

stresses<sup>19</sup>, including mouse rearing facilities with different environmental background in a similar way to the mouse genetic background.

CDK6 does not contain a DNA-binding domain but exerts its effects by interacting with transcription factors. We have identified the transcription factors with which CDK6 interacts to determine HSC self-renewal. In line with our data on leukemic cells,<sup>10</sup> CDK6 interacts with NFY-A in a kinase-dependent manner. The CDK6-NFY-A complex induces a gene set that characterizes activated HSCs. CDK6 and CDK2 phosphorylate the DNA-binding domain of NFY-A<sup>10,33,34</sup>. We have shown that CDK6 interacts with NFY-A in *Cdk6*<sup>+/+</sup> and *Cdk6*<sup>KM/KM</sup> HSPCs. We postulate that kinase-inactivated CDK6 inhibits NFY-A by interacting with it and preventing its phosphorylation, thereby blocking the transcription of NFY-A-dependent genes and suppressing the progression of HSCs to activated MPP1 cells. Knocking down NFY-A in HSCs with kinase inactivated CDK6 leads to an increase in apoptosis, which was not seen in HSCs with wildtype or lacking CDK6. This might be explained by the fact that both proteins regulate p53-response<sup>10,24,25</sup> and underline the importance of the delicate axis of CDK6 and NFY-A in activated progenitor cells.

The transcription pattern of *Cdk6*<sup>KM/KM</sup> HSCs upon transplantation directs the cells to a more quiescent state. The HSC maintenance axis is characterized by a regulating complex including CDK6 and MAZ. The critical role of kinase inactivated CDK6 and MAZ interaction is supported by MAZ knockdown experiments in HSCs, as HSCs lose their self-renewal ability.

ChIP-Seq data of CDK6 and MAZ from leukemic B cells reveal a large set of common target genes, showing that the role of CDK6 and MAZ is not restricted to healthy hematopoietic cells. We speculate that the effect on MAZ might be due to a scaffolding function or to the blockage of certain phosphorylation sites that are critical for transcriptional inactivation or chromatin release. Similar to CTCF, MAZ interacts with a subset of cohesins to organize the chromatin<sup>35</sup>.

The transcription factor MAZ provides another possibility to balance differentiation. MAZ binds the promoters of genes related to erythroid differentiation. It is highly expressed in several cancers and regulates angiogenesis via VEGF, another known CDK6 target<sup>7,9,36–39</sup>. MAZ is also a cofactor of CTCF in embryonic stem cells, where it insulates active chromatin at *Hox* clusters during differentiation<sup>37</sup>. This function could explain the bias towards myeloid-directed differentiation in *Cdk6*<sup>KM/KM</sup> HSPCs, which suggests that CDK6 regulates *Hox* genes and thereby differentiation together with MAZ and CTCF. We thus have evidence for a role of CDK6 in regulation not only in the most naïve HSC compartment but also in early hematopoietic progenitors.

Our data point at a regulation of NFY-A and MAZ by CDK6 which is important for the long-term repopulation capability of HSCs. Our results present a strategy to enhance the success of HSCTs by pre-treating HSCs with CDK4/6 kinase inhibitors. CDK4/6 kinase inhibitors are used and tested for combinatorial cancer therapy<sup>7,40</sup>. These treatments might bring an advantage for healthy HSC fitness as a bystander of cancer therapy. We highlight CDK6 as a major player in HSPCs and inactivation of the CDK6 kinase domain thus has dramatically different consequences to loss of CDK6. In regards of the upcoming protein degrader strategies, it is key to consider our data on HSCs lacking CDK6, showing a reduced HSC potential for, any clinical trials.

**Acknowledgements:** The authors thank M. Ensfelder-Koperek, P. Kudweis, S. Fajmann, P. Jodl, D. Werdenich and I. Dhrami for excellent technical support; G. Tebb for his excellent knowledge and support in scientific writing; M. Milsom and F. Grebien for scientific discussions; U. Ma for great technical support and the FACS facility MedUni Vienna for experimental support; The Biomedical Sequencing Facility (BSF) at CeMM for NGS library preparation, sequencing, and related bioinformatics analyses; This research was supported using resources of the VetCore Facility (Mass Spectrometry) of the University of Veterinary Medicine Vienna. Graphics were created with BioRender.com

**Authorship contributions:** Conceptualization, I.M.M., T.K., E.D., V.S., K.K.; formal analysis, T.K., M.Z., R.G., G.H.; performing experiments I.M.M., E.D., S.K., L.G., M.P-M., A.S., M.F.; technical support U.M., L.E.S., N.K; resources: M.M.; A.F., E.Z-B.; writing, I.M.M., E.D., T.K., K.K.; supervision, V.S., K.K.

**Disclosure of Conflicts of Interest:** The authors declare no competing interests.

**Funding:** This work was supported by the European Research Council (ERC) under the European Union's Horizon 2020 research and innovation program grant agreement No 694354. This research was funded in whole or in part by the Austrian Science Fund (FWF) [SFB-F6101, P 31773]. For open access purposes, the author has applied a CC BY public copyright license to any author-accepted manuscript version arising from this submission.

## References

1. Orkin SH, Zon LI. Hematopoiesis: An Evolving Paradigm for Stem Cell Biology. *Cell*. 2008;132(4):631–644.
2. Wilson A, Laurenti E, Oser G, et al. Hematopoietic Stem Cells Reversibly Switch from Dormancy to Self-Renewal during Homeostasis and Repair. *Cell*. 2008;135(6):1118–1129.
3. Mayer IM, Hoelbl-Kovacic A, Sexl V, Doma E. Isolation, Maintenance and Expansion of Adult Hematopoietic Stem/Progenitor Cells and Leukemic Stem Cells. *Cancers*. 2022;14(7):1723.
4. Bazinet A, Popradi G. A General Practitioner's Guide to Hematopoietic Stem-cell Transplantation. *Current Oncology*. 2019;26(3):187–191.
5. Yanada M. The evolving concept of indications for allogeneic hematopoietic cell transplantation during first complete remission of acute myeloid leukemia. *Bone Marrow Transplant*. 2021;56(6):1257–1265.
6. Laurenti E, Göttgens B. From haematopoietic stem cells to complex differentiation landscapes. *Nature*. 2018;553(7689):418–426.
7. Nebenfuehr S, Kollmann K, Sexl V. The role of CDK6 in cancer. *Int. J. Cancer*. 2020;147(11):2988–2995.
8. Handschick K, Beuerlein K, Jurida L, et al. Cyclin-Dependent Kinase 6 Is a Chromatin-Bound Cofactor for NF-κB-Dependent Gene Expression. *Molecular Cell*. 2014;53(4):682.
9. Kollmann K, Heller G, Schneckenleithner C, et al. A Kinase-Independent Function of CDK6 Links the Cell Cycle to Tumor Angiogenesis. *Cancer Cell*. 2013;24(2):167–181.
10. Bellutti F, Tigan A-S, Nebenfuehr S, et al. CDK6 Antagonizes p53-Induced Responses during Tumorigenesis. *Cancer Discov*. 2018;8(7):884–897.
11. Uras IZ, Maurer B, Nivarthi H, et al. CDK6 coordinates JAK2V617F mutant MPN via NF-κB and apoptotic networks. *Blood*. 2019; 11;133(15):1677–1690
12. Klein K, Witalisz-Siepracka A, Gotthardt D, et al. T Cell-Intrinsic CDK6 Is Dispensable for Anti-Viral and Anti-Tumor Responses In Vivo. *Front. Immunol*. 2021;12:650977.
13. Scheicher R, Hoelbl-Kovacic A, Bellutti F, et al. CDK6 as a key regulator of hematopoietic and leukemic stem cell activation. *Blood*. 2015;125(1):90–101.
14. Hu MG, Deshpande A, Schlichting N, et al. CDK6 kinase activity is required for thymocyte development. *Blood*. 2011;117(23):6120–6131.
15. Malumbres M, Sotillo R, Santamaría D, et al. Mammalian Cells Cycle without the D-Type Cyclin-Dependent Kinases Cdk4 and Cdk6. *Cell*. 2004;118(4):493–504.
16. Giladi A, Paul F, Herzog Y, et al. Single-cell characterization of haematopoietic progenitors and their trajectories in homeostasis and perturbed haematopoiesis. *Nat Cell Biol*. 2018;20(7):836–846.
17. Rodriguez-Fraticelli AE, Weinreb C, Wang S-W, et al. Single-cell lineage tracing unveils a role for TCF15 in haematopoiesis. *Nature*. 2020;583(7817):585–589.
18. Venezia TA, Merchant AA, Ramos CA, et al. Molecular Signatures of Proliferation and Quiescence in Hematopoietic Stem Cells. *PLoS Biol*. 2004;2(10):e301.
19. Kanayama M, Izumi Y, Yamauchi Y, et al. CD86-based analysis enables observation of bona fide hematopoietic responses. *Blood*. 2020;136(10):1144–1154.
20. Ito K, Turcotte R, Cui J, et al. Self-renewal of a purified *Tie2*<sup>+</sup> hematopoietic stem cell population relies on mitochondrial clearance. *Science*. 2016;354(6316):1156–1160.
21. Arai F, Hirao A, Ohmura M, et al. Tie2/Angiopoietin-1 Signaling Regulates Hematopoietic Stem Cell Quiescence in the Bone Marrow Niche. *Cell*. 2004;118(2):149–161.

22. Cabezas-Wallscheid N, Klimmeck D, Hansson J, et al. Identification of Regulatory Networks in HSCs and Their Immediate Progeny via Integrated Proteome, Transcriptome, and DNA Methylome Analysis. *Cell Stem Cell*. 2014;15(4):507–522.
23. Doma E, Mayer IM, Brandstetter T, et al. A robust approach for the generation of functional hematopoietic progenitor cell lines to model leukemic transformation. *Blood Advances*. 2021;5(1):39–53.
24. Gatta R, Dolfini D, Mantovani R. NF-Y joins E2Fs, p53 and other stress transcription factors at the apoptosis table. *Cell Death Dis*. 2011;2(5):e162–e162.
25. Bungartz G, Land H, Scadden DT, Emerson SG. NF-Y is necessary for hematopoietic stem cell proliferation and survival. *Blood*. 2012;119(6):1380–1389.
26. Pinto do O P. Expression of the LIM-homeobox gene LH2 generates immortalized Steel factor-dependent multipotent hematopoietic precursors. *The EMBO Journal*. 1998;17(19):5744–5756.
27. Yue F, Cheng Y, Breschi A, et al. A comparative encyclopedia of DNA elements in the mouse genome. *Nature*. 2014;515(7527):355–364.
28. Busch K, Klapproth K, Barile M, et al. Fundamental properties of unperturbed haematopoiesis from stem cells in vivo. *Nature*. 2015;518(7540):542–546.
29. Bisi JE, Sorrentino JA, Jordan JL, et al. Preclinical development of G1T38: A novel, potent and selective inhibitor of cyclin dependent kinases 4/6 for use as an oral antineoplastic in patients with CDK4/6 sensitive tumors. *Oncotarget*. 2017;8(26):42343–42358.
30. Lapidot T, Dar A, Kollet O. How do stem cells find their way home? *Blood*. 2005;106(6):1901–1910.
31. He S, Roberts PJ, Sorrentino JA, et al. Transient CDK4/6 inhibition protects hematopoietic stem cells from chemotherapy-induced exhaustion. *Sci. Transl. Med*. 2017;9(387):eaal3986.
32. Laurenti E, Frelin C, Xie S, et al. CDK6 Levels Regulate Quiescence Exit in Human Hematopoietic Stem Cells. *Cell Stem Cell*. 2015;16(3):302–313.
33. Farina A, Manni I, Fontemaggi G, et al. Down-regulation of cyclin B1 gene transcription in terminally differentiated skeletal muscle cells is associated with loss of functional CCAAT-binding NF-Y complex. *Oncogene*. 1999 6;18(18):2818–27.
34. Yun J, Chae H-D, Choi T-S, et al. Cdk2-dependent Phosphorylation of the NF-Y Transcription Factor and Its Involvement in the p53-p21 Signaling Pathway. *Journal of Biological Chemistry*. 2003;278(38):36966–36972.
35. Xiao T, Li X, Felsenfeld G. The Myc-associated zinc finger protein (MAZ) works together with CTCF to control cohesin positioning and genome organization. *Proc. Natl. Acad. Sci. U.S.A.* 2021;118(7):e2023127118.
36. Deen D, Butter F, Daniels DE, et al. Identification of the transcription factor MAZ as a regulator of erythropoiesis. *Blood Advances*. 2021;5(15):3002–3015.
37. Ortabozkoyun H, Huang P-Y, Cho H, et al. CRISPR and biochemical screens identify MAZ as a cofactor in CTCF-mediated insulation at Hox clusters. *Nat Genet*. 2022;54(2):202–212.
38. Triner D, Castillo C, Hakim JB, et al. Myc-Associated Zinc Finger Protein Regulates the Proinflammatory Response in Colitis and Colon Cancer via STAT3 Signaling. *Molecular and Cellular Biology*. 2018;38(22):e00386–18.
39. Yu Z-H, Lun S-M, He R, et al. Dual function of MAZ mediated by FOXF2 in basal-like breast cancer: Promotion of proliferation and suppression of progression. *Cancer Letters*. 2017;402:142–152.
40. Fassl A, Geng Y, Sicinski P. CDK4 and CDK6 kinases: From basic science to cancer therapy. *Science*. 2022;375(6577):eabc1495.



538

539

## Figure legends

### Figure 1: CDK6 shapes the HSC transcriptomic landscape in a kinase-inactivated, kinase -dependent and -independent manner

(A) Flow cytometry analysis of isolated BM from *Cdk6*<sup>+/+</sup>, *Cdk6*<sup>-/-</sup> and *Cdk6*<sup>KM/KM</sup> mice. Cell numbers of HSCs (LSK [Lin<sup>-</sup>Sca-1<sup>+</sup>c-kit<sup>+</sup>] CD34<sup>-</sup>CD48<sup>-</sup>CD150<sup>+</sup>CD135<sup>-</sup>), MPP1 (LSK CD34<sup>+</sup>CD48<sup>-</sup>CD150<sup>+</sup>CD135<sup>-</sup>), MPP2 (LSK CD48<sup>+</sup>CD150<sup>+</sup>) and MPP3/4 (LSK CD48<sup>+</sup>CD150<sup>-</sup>), (n = 10; mean ± standard error of the mean [SEM]). (B) (top) Experimental scheme of 10X Genomics scRNA-seq including flow cytometry sorting of LSK cells of *Cdk6*<sup>+/+</sup>, *Cdk6*<sup>-/-</sup> and *Cdk6*<sup>KM/KM</sup> BM. (bottom) Uniform Manifold Approximation and Projection (UMAP) visualization of 11 LSK cell clusters. Colours indicate different clusters. HSPC: Hematopoietic stem and progenitor cell, Cycle: Cell cycle, Myel: Myeloid, Lym: Lymphoid, Rep: Replication (C) UMAP of 9 HSPC subclusters with colour code. MPP: Multipotent progenitor, IFN: Interferon, Ery: Erythroid. (D) Bar chart of HSPC subcluster size differences of either *Cdk6*<sup>-/-</sup> or *Cdk6*<sup>KM/KM</sup> compared to *Cdk6*<sup>+/+</sup> control (Log<sub>2</sub>FC of % cluster sizes relative to *Cdk6*<sup>+/+</sup>). (E) UMAP of *Cdk6*<sup>+/+</sup>, *Cdk6*<sup>-/-</sup> and *Cdk6*<sup>KM/KM</sup> HSPC cluster. Arrow indicates HSC subcluster. (F) (top) Nomenclature of kinase-inactivated, kinase-dependent and loss of CDK6. (bottom) Venn diagrams showing number of genes of the HSC subcluster uniquely or commonly upregulated (left) / downregulated (right) in *Cdk6*<sup>KM/KM</sup> and *Cdk6*<sup>-/-</sup> compared to *Cdk6*<sup>+/+</sup> (|Log<sub>2</sub>FC| ≥ 0.3). (G) UMAP showing *Cdk6*<sup>+/+</sup>, *Cdk6*<sup>-/-</sup> and *Cdk6*<sup>KM/KM</sup> HSPCs overlayed with the HSC associated proliferation gene signature (Psig)<sup>18</sup>. The 15% of cells with the lowest Psig score (compare methods) are indicated in blue. Violin plots depicting Psig and HSC associated quiescent signature (Qsig) of all three genotypes.

## Figure 2: Kinase-inactivated CDK6 maintains HSPC potential upon long-term challenge

(A) Experimental workflow of repetitive *in vivo* pI:pC injections followed by an *in vitro* serial plating assay of *Cdk6*<sup>+/+</sup>, *Cdk6*<sup>-/-</sup> and *Cdk6*<sup>KM/KM</sup> BM cells. (B) Flow cytometry analysis of L<sup>-</sup>K<sup>+</sup>CD86<sup>+</sup> and HSC-MPP1 (from L<sup>-</sup>K<sup>+</sup>CD86<sup>+</sup>) cells upon serial pI:pC injection (n ≥ 3, mean ± SEM). (C) Cell cycle distribution of HSC/MPP1 cells upon serial pI:pC treatment (n=5, mean ± SEM). (D) Representative flow cytometry plots showing serially plated LSK cells upon repetitive pI:pC treatment. (SP: serial plating) (E) Relative quantification of LSK cells during serial plating after repetitive *in vivo* pI:pC treatment (n = 3-6, mean ± SEM).

## Figure 3: Kinase-inactivated CDK6 enhances HSC homing and self-renewal

(A) Top upregulated genes in dormant *Cdk6*<sup>KM/KM</sup> HSCs compared to *Cdk6*<sup>+/+</sup> and *Cdk6*<sup>-/-</sup> cells from scRNA-seq. (B) Schematic representation of BM homing assay *in vivo*. (C) Flow cytometry analysis of homed CD45.2<sup>+</sup> *Cdk6*<sup>+/+</sup>, *Cdk6*<sup>-/-</sup> and *Cdk6*<sup>KM/KM</sup> LSK and HSC/MPP1 of LSK cells 18h post-injection into CD45.1<sup>+</sup> recipients (n ≥ 11 recipients and donors, mean ± SEM). (D) Serial BM transplantation workflow of *Cdk6*<sup>+/+</sup>, *Cdk6*<sup>-/-</sup> and *Cdk6*<sup>KM/KM</sup> BM cells. (E) Representative flow cytometry plots of gated LSK cells over four rounds of transplantation (TP). (F, G) % of engrafted CD45.2<sup>+</sup> *Cdk6*<sup>+/+</sup>, *Cdk6*<sup>-/-</sup> and *Cdk6*<sup>KM/KM</sup> LSK and HSC/MPP1 cells over four rounds of transplantation. (H) Lineage distribution of engrafted CD45.2<sup>+</sup> *Cdk6*<sup>+/+</sup>, *Cdk6*<sup>-/-</sup> and *Cdk6*<sup>KM/KM</sup> BM cells (n = 3-6/genotype, mean ± SEM). (I) Experimental design competitive BM transplantation assay, depicting 1:1 ratio transplantation of CD45.1<sup>+</sup> *Cdk6*<sup>+/+</sup> together with either CD45.2<sup>+</sup> *Cdk6*<sup>+/+</sup> or *Cdk6*<sup>KM/KM</sup> BM into lethally irradiated recipient mice. (J) Endpoint analysis of competitive transplantation showing CD45.2<sup>+</sup> *Cdk6*<sup>+/+</sup> and *Cdk6*<sup>KM/KM</sup> HSC/MPP1 cells (n = 7/group, mean ± SEM).

## Figure 4: Kinase-inactivated CDK6 balances quiescent and activated transcriptional programs of long-term HSCs

(A) Experimental workflow of low-input RNA-seq of engrafted CD45.2<sup>+</sup> HSC/MPP1 cells after two serial rounds of transplantation. (B) Venn diagrams showing genes uniquely or commonly upregulated (left) / downregulated (right) in *Cdk6*<sup>-/-</sup> and *Cdk6*<sup>KM/KM</sup> compared to *Cdk6*<sup>+/+</sup> HSC/MPP1 cells after two serial rounds of transplantation (n=3, |Log<sub>2</sub>FC| ≥ 0.3, adjusted p-value < 0.2). (C, D) Gene set enrichment analysis (GSEA) to test for the enrichment of quiescent or activated stem cell gene sets in differentially expressed genes coming from three analyses: HSC/MPP1 cells of *Cdk6*<sup>KM/KM</sup> in comparison to *Cdk6*<sup>+/+</sup> cells, *Cdk6*<sup>KM/KM</sup> compared to *Cdk6*<sup>-/-</sup> or *Cdk6*<sup>-/-</sup> compared to *Cdk6*<sup>+/+</sup> after two serial rounds of transplantation. (E, F) Transcription factor motif enrichment analysis of genes within the activated stem cell gene set that are either upregulated in (E) *Cdk6*<sup>KM/KM</sup> compared to *Cdk6*<sup>+/+</sup> HSC/MPP1 cells or (F) *Cdk6*<sup>-/-</sup> compared to *Cdk6*<sup>+/+</sup> HSC/MPP1 cells upon two serial rounds of transplantation. (G) Subcellular fractionation of *Cdk6*<sup>+/+</sup>, *Cdk6*<sup>-/-</sup> and *Cdk6*<sup>KM/KM</sup> HPC<sup>LSK</sup> cells, followed by western blot analysis of CDK6. Lamin B1/RCC1 served as nuclear, while HSP-90 as a cytoplasmic marker. (H) Anti-NFY-A co-immunoprecipitation (co-IP) from HPC<sup>LSK</sup> *Cdk6*<sup>+/+</sup>, *Cdk6*<sup>-/-</sup> and *Cdk6*<sup>KM/KM</sup> cell extracts followed by NFY-A and CDK6 immunoblotting. IN indicates the input lysate and SN indicates the supernatant after IP. GAPDH served as loading control.

## Figure 5: Kinase-inactivated CDK6 and MAZ influence HSC maintenance

(A-B) Transcription factor motif enrichment analysis of genes within the quiescence stem cell gene set that are either upregulated in (A) *Cdk6*<sup>KM/KM</sup> compared to *Cdk6*<sup>+/+</sup> cells or (B) *Cdk6*<sup>-/-</sup> compared to *Cdk6*<sup>+/+</sup> cells after two serial rounds of transplantation. (C) CDK6 interactome analysis generated by nuclear CDK6-IP mass spectrometry analysis of HPC-7 cell lines expressing either wildtype CDK6 or CDK6<sup>KM</sup>. Dot plot illustrating all protein interactions with CDK6 or CDK6<sup>KM</sup> vs. CDK6<sup>-/-</sup> (Log<sub>2</sub>FC). Established CDK6 interactors are highlighted in blue. Transcription factors interacting with CDK6<sup>KM</sup> and analyzed from the CDK6<sup>KM</sup>

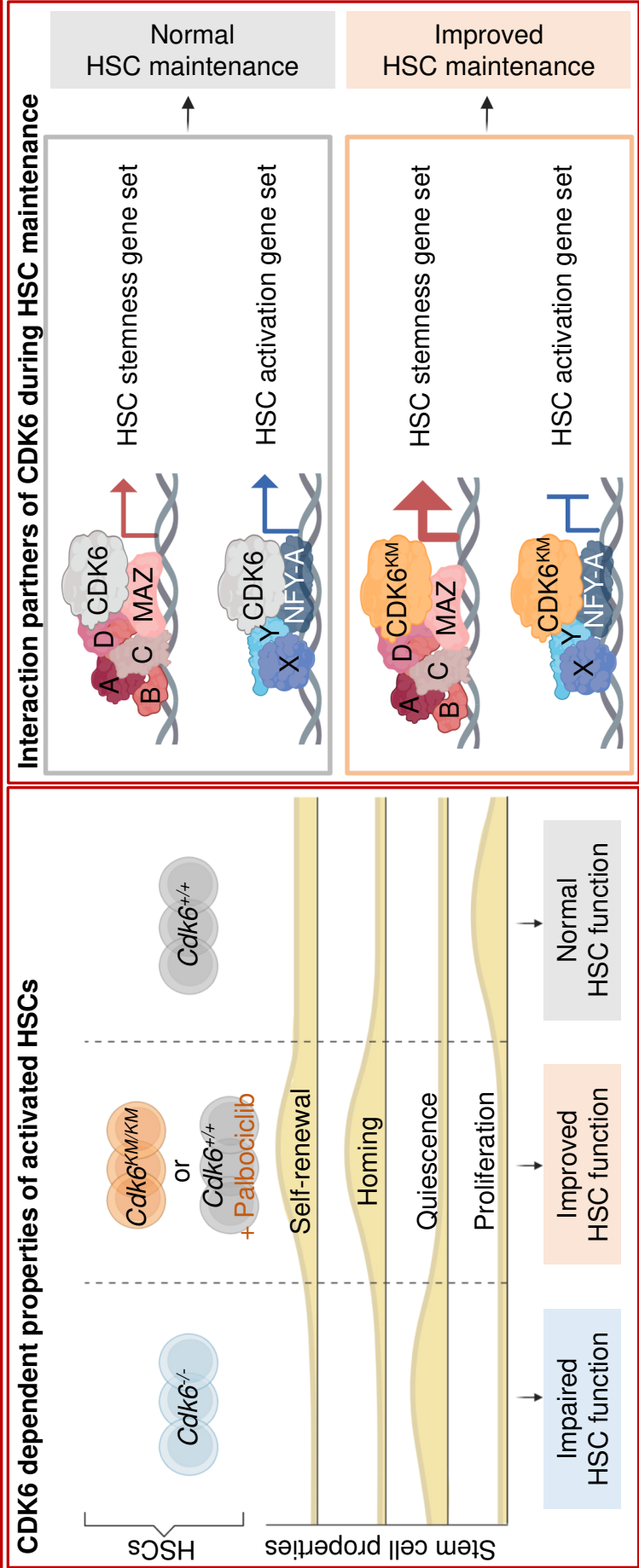
specific motif analysis from Fig. S5A are highlighted in red. **(D)** Flow cytometry proximity ligation assay of CDK6 and MAZ antibodies showing endogenous protein interaction in *ex vivo* *Cdk6*<sup>+/+</sup>, *Cdk6*<sup>-/-</sup> and *Cdk6*<sup>KM/KM</sup> HSC/MPP1 cells. Representative flow cytometry histograms are depicted on the right. *Cdk6*<sup>-/-</sup> cells, MAZ and CDK6 antibody only samples served as controls. **(E)** Overlap of CDK6 ChIP-seq data from BCR/ABL<sup>p185+</sup> cells with published MAZ ChIP-seq data from CH12.LX mouse lymphoma cell line. **(F)** Annotation of the genomic regions identified in the CDK6/MAZ ChIP-seq overlap. **(G)** CDK6/MAZ ChIP-seq overlay (+2kb- -500b to TSS) with upregulated genes of *Cdk6*<sup>KM/KM</sup> compared to *Cdk6*<sup>+/+</sup> dormant HSC subcluster genes (scRNA-seq FC ≥ 0.3). **(H)** Stem cell genes of *Cdk6*<sup>KM/KM</sup> or *Cdk6*<sup>-/-</sup> cells compared to *Cdk6*<sup>+/+</sup> cells with a CDK6-MAZ ChIP peak. **(I)** Experimental design of siRNA MAZ knockdown assay +/- Palbociclib treatment in sorted LSK cells of *Cdk6*<sup>+/+</sup> and *Cdk6*<sup>KM/KM</sup> mice. **(J, K)** Flow cytometry analysis of **(J)** HSC/MPP1 scramble cells and **(K)** HSC/MPP1 cells of LSK cells upon MAZ knockdown +/- Palbociclib treatment depicted as Log<sub>2</sub>FC relative to corresponding scramble controls (n = 4 per genotype, mean ± SEM).

## **Figure 6: CDK4/6 kinase inhibition protects HSC fitness**

**(A)** Experimental scheme of 10X Genomics scRNA-seq including flow cytometry sorting of LSK cells followed by 24h cultivation with either PBS or Palbociclib. **(B)** UMAP visualization of 13 LSK cell clusters. Colours indicate different clusters. Neutro: Neutrophil, Dendr: Dendritic, Cycle: Cell cycle, M/L Cycle: Myeloid/Lymphoid cell cycle, Innate: Innate lymphocyte, MK: Megakaryocyte, Ribos: Ribosomes, HSPC: Hematopoietic stem and progenitor cell, Ery: Erythroid, Granu: Granulocyte, D/M: Dendritic/Macrophage. **(C)** UMAP of 4 HSPC subclusters. Myel 1: Myeloid (Granulocyte), Myel 2: Dendritic, Myel 3: Neutrophil, Naïve: Immature cells. **(D)** Bar chart of relative HSPC subcluster sizes of the PBS or Palbociclib treated samples. **(E)** Heatmap of top 50 upregulated genes upon Palbociclib

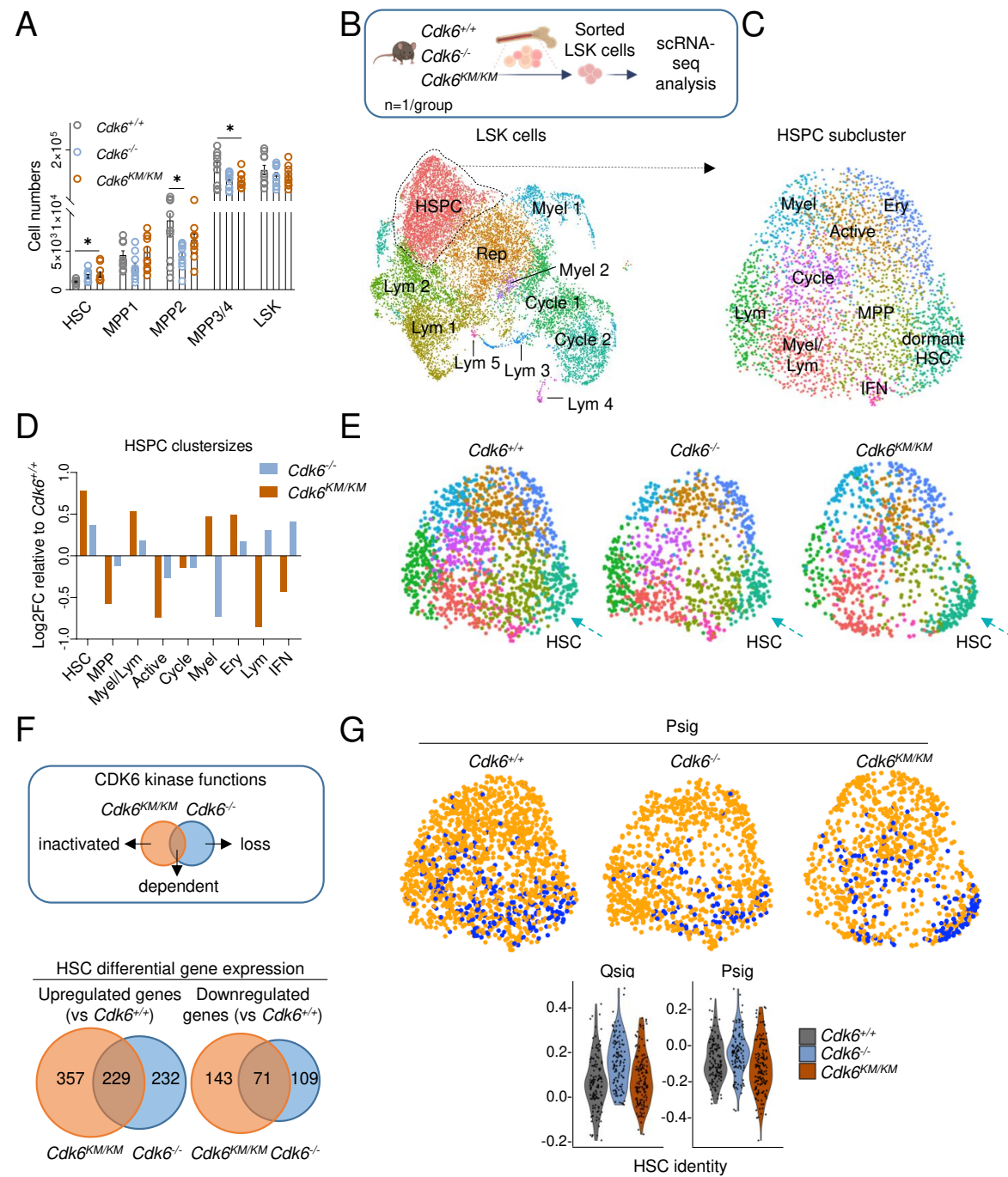
treatment compared to control out of the 282 genes found in Fig. 5G. Errors indicate top genes of Fig. 5H, also found in the Palbociclib comparison. **(F)** Experimental design to assess *in vivo* Palbociclib treatment followed by an *in vitro* serial plating assay of sorted HSC/MPP1 cells. **(G)** Flow cytometry analysis of HSC/MPP1 cells and **(H)** serially plated LSK cell numbers upon *in vivo* Palbociclib treatment ( $n \geq 4$ , mean  $\pm$  SEM). **(I)** Experimental design for competitive BM transplantation assay. CD45.1<sup>+</sup> control and Palbociclib treated (200nM) CD45.2<sup>+</sup> BM cells were transplanted in a 1:1 ratio into lethally irradiated recipient mice upon 72h of cultivation. **(J, K)** Endpoint analysis of engrafted BM LSK and HSC/MPP1 cells upon Palbociclib treatment ( $n = 7/\text{group}$ , mean  $\pm$  SEM). **(L)** Experimental overview of PBS or Palbociclib treated human CD34<sup>+</sup> cells followed by a serial plating assay. **(M, N)** Percentage of CD34<sup>+</sup>CD38<sup>-</sup> cells and mean fluorescence intensity [MFI] of CD34<sup>+</sup> cells in 2 serial plating rounds ( $n = 3-4/\text{treatment}$ , mean  $\pm$  SEM).

# Kinase inactivated CDK6 in long-term HSC functionality



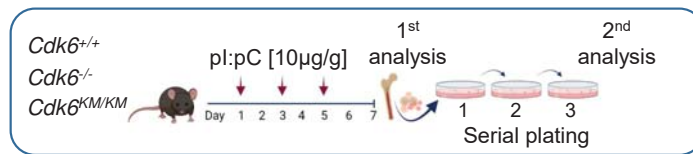
**Conclusion:** CDK6 balances self-renewal, homing, quiescence and proliferation in activated HSCs. Inhibiting CDK6 kinase function enhances long-term HSC functionality by a complex including CDK6 and MAZ, which activates an HSC maintenance specific transcriptional pattern.

Mayer et al. DOI



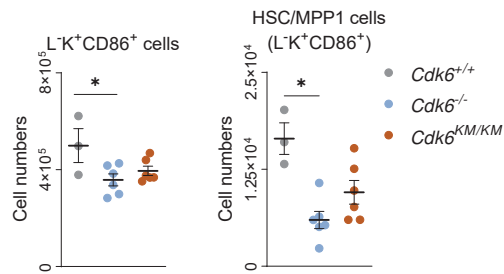


A

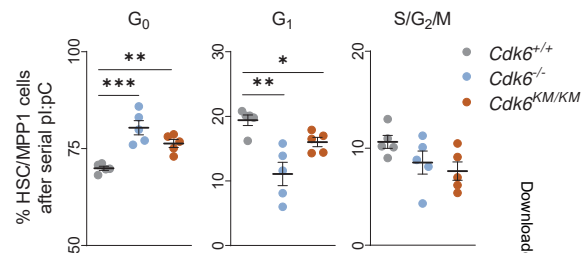


B

1<sup>st</sup> analysis:

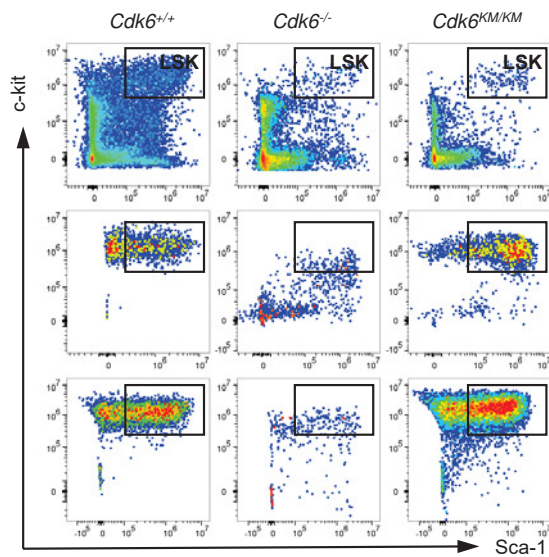


C

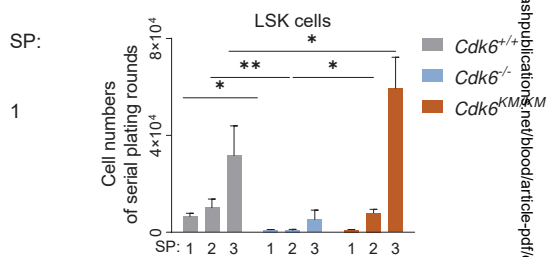


D

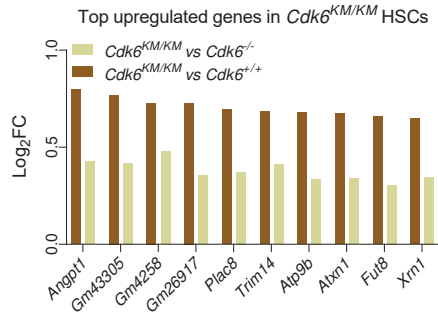
2<sup>nd</sup> analysis:



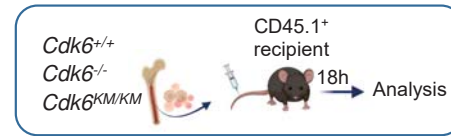
E



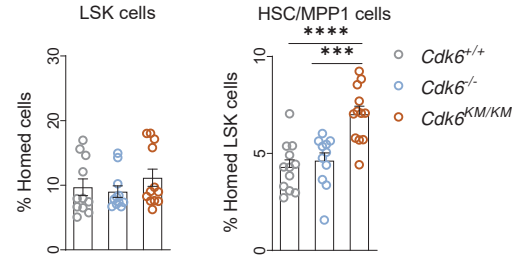
A



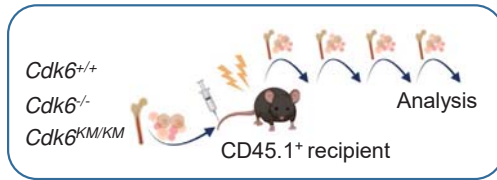
B



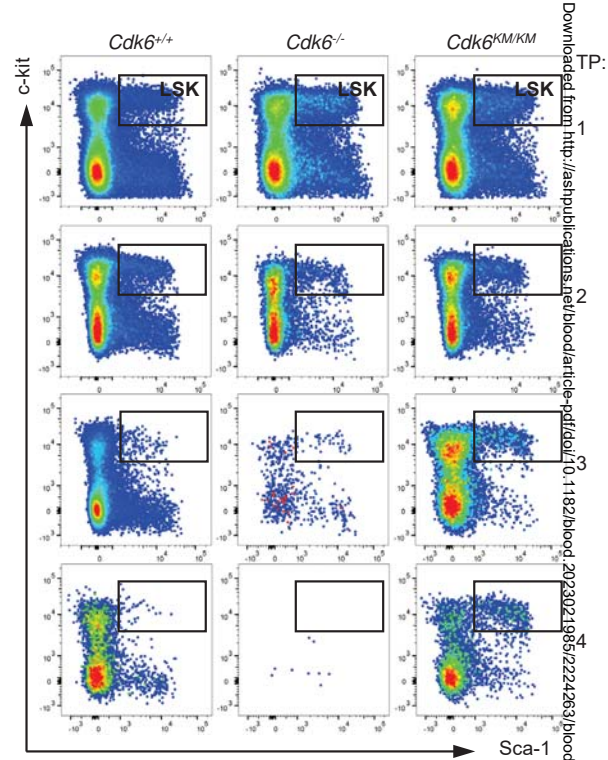
C



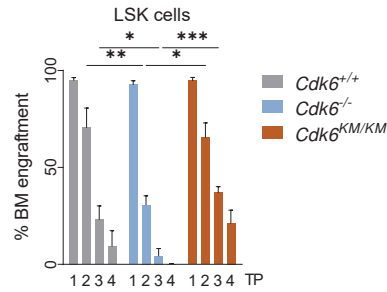
D



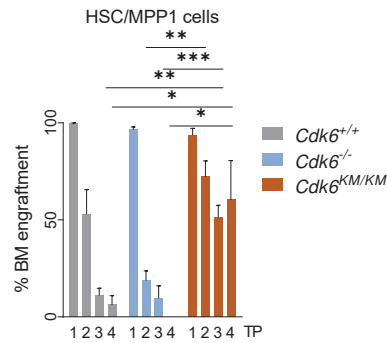
E



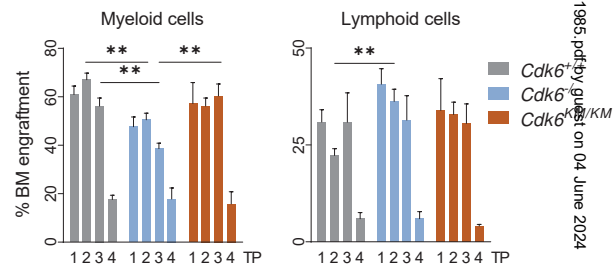
F



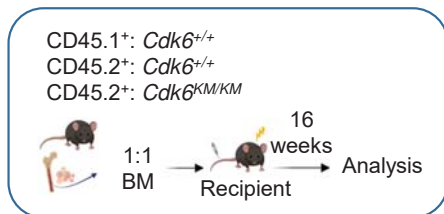
G



H



I



J

